Hindawi
Advances in Polymer Technology
Volume 2022, Article ID 3513804, 11 pages
https://doi.org/10.1155/2022/3513804

Research Article

Investigations of the Elongational Deformation Induced by Pins in Pin-Barrel Cold-Feed Extruders

Zhilin Wang, Yiren Pan, Yanchang Liu, Jing Huang, Ning Wang, and Xuehua Hu

Institute of Mechanical and Electrical Engineering, Qingdao University of Science and Technology, Qingdao, Shandong 266061, China

Correspondence should be addressed to Yanchang Liu; jnelyc@126.com

Received 29 September 2021; Revised 13 January 2022; Accepted 27 January 2022; Published 27 February 2022

Academic Editor: Alain Durand

This paper is a study on the elongational deformation induced by pins in pin-barrel cold-feed extruders. The mathematical model is established by using simple flow field, plate model, and Newton constitutive relation. It is proved that there is elongational deformation when the fluid bypasses the pin, and the elongational deformation is quantitatively calculated. The finite element method is used to simulate the flow field of the screw mixing section of the pin-barrel cold-feed extruder with different specifications. The velocity vector nephogram in the simulation results is analyzed by numerical analysis of elongational deformation and compared with the theoretical elongational deformation value. The results show that the simulated and theoretical values of elongational deformation are approximately consistent. The numerical analysis of the key factors affecting the elongational deformation shows that the elongational deformation will gradually increase with the increase of screw diameter. For the screw of the same specification, the increasing helical angle will reduce the elongational deformation, and the increasing rotational speed will linearly increase the elongational deformation in unit time. This study can be used to roughly estimate the elongational deformation induced by pins and establish the mixing theoretical model of the pin-barrel cold-feed extruder.

1. Introduction

Since its birth in 1972, the pin-barrel cold-feed extruder has been paid more and more attention by rubber industry, especially by tire manufacturers. Because of its relatively strong mixing performance, it has been widely used in rubber extrusion process. The structural characteristics of the pin-barrel cold-feed extruder are that 6~10 rows of pins are installed on the barrel and 6~12 pins are arranged on each row of pins (Figure 1) [1]. The number and rows of pins depend on the diameter and length-diameter ratio of the screw. The main role of barrel pins is to continuously conduct (i) diversion orientation, (ii) elongational deformation, and (iii) position replacement for high viscosity rubber, which greatly promotes the interface growth, enhances the distribution mixing, improves the plasticization (softening) efficiency, and achieves the requirements of deformation and temperature uniformity [2–5, 23, 24].

Many experimental and simulation studies have been carried out on the mixing behavior of pin-barrel cold-feed extruder [6–10]. Yabushita et al. used a white compound and a black compound to study the mixing performance of pin barrel extruder with two rows of pins and ordinary cold-feed extruder. Their contrastive experimental results showed that the introduction of pins could greatly improve the distribution mixing effect [6]. Shin and White used the flow analysis network method to study the influence of introducing slots in the screw flights and pins on the barrel on the screw pump characteristics. Their analysis results showed that the slots in the screw flights reduced the pumping capacity and the pumping capacity of the two extruders was very close [7]. Brzoskowski et al., through the establishment of kinematic model and the use of flow network analysis method, concluded that the reorientation and elongation of the rubber compounds induced by pin movement were the key factors to obtain good mixing effect [8].

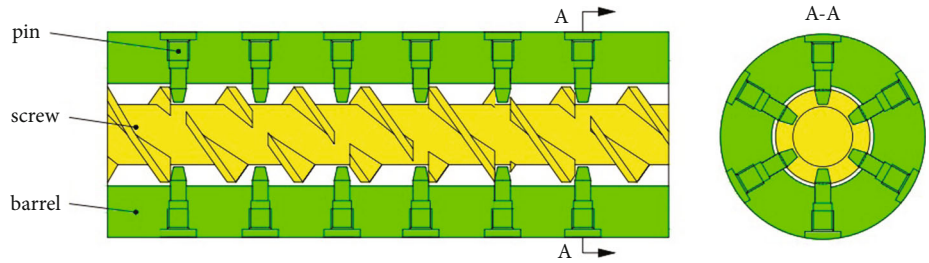

Figure 1: Pin barrel section.

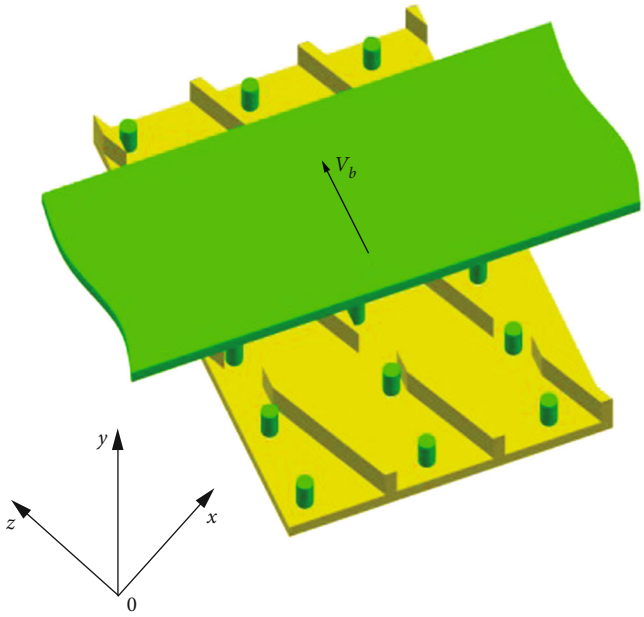

Figure 2: Flat plate model with a stationary screw and a moving barrel.

Schöppner et al. tried to optimize the distribution and dispersion mixing effect in the screw channel by changing the geometric design and arrangement of pins. Their experimental and simulation results showed that the geometric changes of pins (cylindrical, concave, convex, and conical) had no effect on the dispersion mixing, but they could almost equally greatly enhance the distribution mixing effect [9].

However, the mixing theory of pin-barrel cold-feed extruder still lags far behind the engineering practice, because, so far, a complete mathematical model of mixing behavior of pin-barrel cold-feed extruder has not been established. The reason for this is that the flow field in the pin-barrel section is very complex and difficult to model. This condition also includes elongational deformation induced by pins. When the fluid bypasses the pin, the fluid produces elongational deformation under the convergence gap formed by the screw flight and the pin. Due to the increase of interfacial area index caused by elongational deformation, the mixing effect is greatly enhanced. Therefore, it is necessary to carry out theoretical analysis on the elongational deformation induced by pins.

The main purpose of this paper is to supplement the mixing theory of pin-barrel extruder, theoretically verify the elongational flow induced by pins, and quantitatively calculate it. However, according to the current technology, the elongational deformation induced by pins cannot be measured by experiments. Therefore, this paper attempts to compare the established simple approximate mathematical model of elongational deformation induced by pins with Polyflow simulation results. The idea of establishing such a model is without considering the precise and complex flow field in the screw channel of the pin barrel section; the existence proof and quantitative calculation of the elongational deformation of the pin are carried out only according to the simple flow field and the screw channel geometry.

2. Mathematical Model

2.1. Motion Transformation and Coordinate Establishment. For the convenience of analysis, the plate approximation and motion transformation are carried out, like the analysis of melt conveying in the extrusion section of single screw extruder [11–13, 22]. That is, the screw channel is unfolded into a flat channel, and the corresponding barrel is unfolded into a flat plate. Suppose the screw is stationary and the barrel rotates. Therefore, in this plate approximation model, the plate (barrel) slides relatively on the developed flat channel (screw channel) (Figure 2). In Figure 2, v_b is the moving speed of the barrel (equal to the linear speed of the screw rotation).

$$v_b = \pi DN, \tag{1}$$

where D is the screw diameter and N is the screw rotational speed.

Under the drag action of the barrel, the velocity of the fluid in the screw channel is decomposed into the cross-channel velocity component v_x and the down-channel velocity component v_z. The coordinate system is established with the cross-channel velocity component direction as x axis, the down-channel velocity component direction as z axis, and the screw channel depth direction as y axis, as shown in Figure 2.

2.2. Basic Equations, Assumptions, and Simplification. In the theoretical analysis, it is assumed that the rubber is incompressible Newtonian fluid and is filled with screw channel. The flow process of the rubber is an isothermal process, so

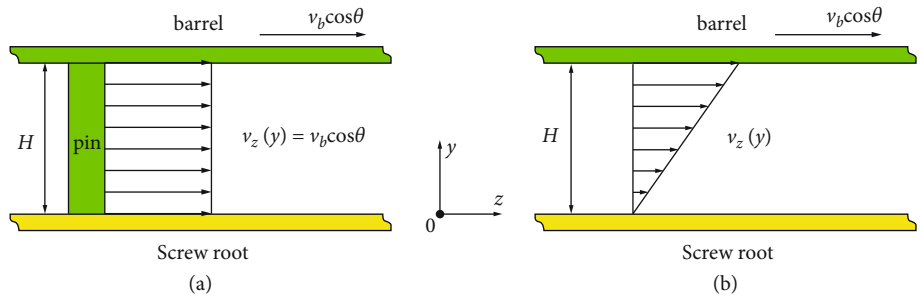

FIGURE 3: Velocity profiles. H is the depth of the screw channel. (a) Pin velocity in the z direction. (b) Fluid z direction velocity in the screw channel area without pins.

the three-dimensional constitutive equation and motion equation of the fluid are the following:

(1) Newton constitutive equation:

$$\tau = -\eta E. \tag{2}$$

(2) Mass conservation equation:

$$\nabla \cdot v = 0. \tag{3}$$

(3) Momentum conservation equation:

$$\rho \frac{Dv}{Dt} = -\nabla P + \eta \nabla^2 v + \rho g, \tag{4}$$

where τ is the stress tensor, η is the Newton viscosity, E is the strain rate tensor, ∇ is the differential operator, v is the velocity vector, ρ is the density, P is the pressure, and g is the gravity acceleration.

Since the viscosity of the rubber increases and the Reynolds value is low,

$$v_y = 0. \tag{5}$$

The v_x has little effect on the elongational deformation induced by pins, so the velocity component v_x can be ignored in the calculation of elongational deformation.

Assuming that the flow along the z direction is a fully developed steady flow and ignores the inertial force, gravity, and pressure gradient along the z direction, the simplified momentum equation in the z direction is

$$\frac{\partial^2 v_z}{\partial y^2} = 0. \tag{6}$$

2.3. Velocity Distribution. In the plate model of Figure 2, the screw channel depth is H. Since the pin is fixed on the barrel and moves together with the random barrel, the velocity of the pin is v_b, which does not change with the change of the height position y of the screw channel (Figure 3(a)).

In the screw channel area without pins, the quadratic integral of Equation (6) is carried out, and the assumption of no wall slip is considered: $y = H, v_z = v_b \cos\theta$; $y = 0, v_z = 0$; get the velocity v_z:

$$v_z(y) = \frac{v_b \cos\theta}{H} y. \tag{7}$$

Therefore, in the screw channel area without pins, the fluid velocity v_z was linearly related to the screw channel height y (Figure 3(b)).

2.4. Generation of Elongational Deformation. As shown in Figure 4, since the typical design value of the ratio $d\cos\theta/W$ of the pin diameter d to the axial width of the screw channel $W/\cos\theta$ is about 0.2, the pin has a noticeable effect on the motion of the fluid in the screw channel. The moment when the pin occupies any position in the screw channel can be seen from Figure 4; due to the geometric constraints of the flight and the pin, the flow channel regions *abgf* and *bcjh* converge geometrically along the z direction. Since the depth of the screw channel is constant, when the fluid flows through these two geometric convergent channels, the linear velocity of the fluid layer will increase at the position y of the same screw channel height. Therefore, in the z direction, for any screw channel height y ($y < H$), the velocity at the cross section along the z direction at the fluid layer lines *fg* and *hj* is greater than that at the lines *ab* and *bc*, respectively. Therefore, there is a velocity gradient in the z direction, resulting in elongational deformation. In Sections 2.5 and 2.6, the existence of the above elongational deformation will be proved, and the elongational deformation will be quantitatively calculated.

2.5. Quantitative Proof of Elongational Deformation. To facilitate the calculation, the pin diameter is approximately equal to the axial width of the screw flight slot. In Figure 4, position "1" is the initial position of the pin movement in a screw channel, position "3" is the end position, and the screw channel region *pqsl* is used as the analysis area of elongational deformation. Position "2" is the position of any pin movement in the analysis area.

Set $\overline{ab} = x_4$, $\overline{bc} = x_2$, $\overline{fg} = x_3$, and $\overline{hj} = x_1$.

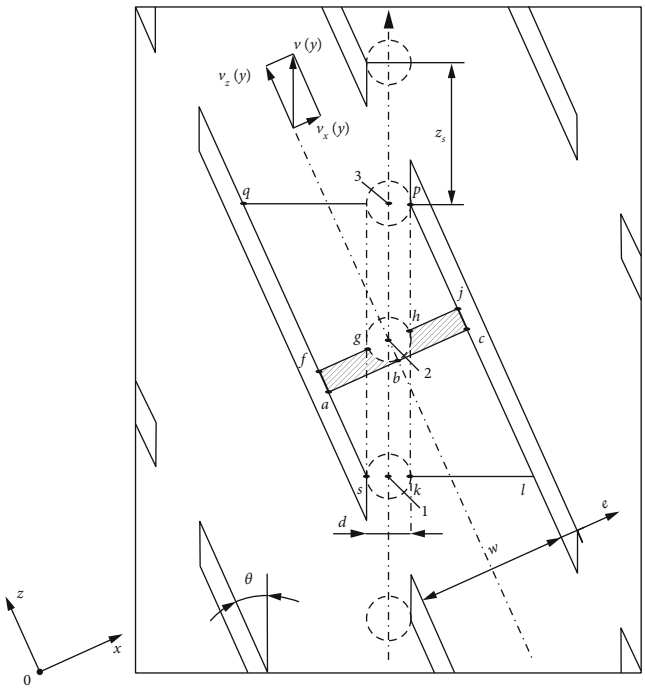

Figure 4: Partially developed view of the cylindrical outer surface of screw for the analysis of elongational deformation induced by pin (θ: helical angle, d: pin diameter, W: normal screw channel width, e: normal screw flight width, z_s: screw flight slot length, and v (y): fluid confluence velocity).

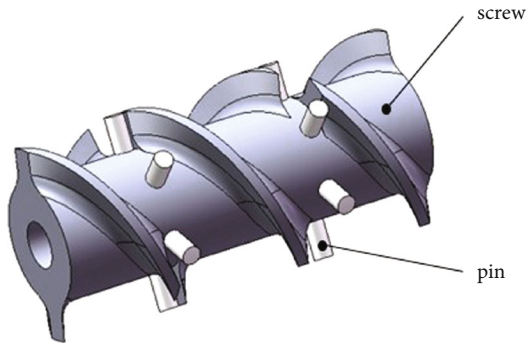

Figure 5: Three-dimensional model of partial pin barrel segment.

When the pin follows the barrel, in the z direction, the interaction of the screw and the pin produces the convergent flow channel. According to the geometric characteristics, it is obvious that

$$x_1 < x_2, \tag{8}$$

$$x_3 < x_4. \tag{9}$$

Let $v_{z1}(y)$, $v_{z2}(y)$, $v_{z3}(y)$, and $v_{z4}(y)$, respectively, be the fluid velocity functions along the z direction on the cross sections of hj, bc, fg, and ab. From the law of conservation of mass, we can obtain

Table 1: Screw specification parameters.

Pin diameter D (mm)	Helical angle θ (°)	Number of pin rows m	Number of pins per row n
65	24	2	6
90	24	2	6
120	24	2	6
150	24	2	6

Table 2: Physical parameters of rubber compound.

Infinite shear viscosity η_∞ (Pa·s)	Zero shear viscosity η_0 (Pa·s)	Relaxation time λ (s)	Non-Newtonian index n
0	$10e+006$	1	0.3

Table 3: Boundary conditions and motion parameters.

Pin diameter D (mm)	Maximum rotational speed N (rpm)	Output capacity Q (kg/h)	Volume flow rate V (m^3/s)
65	80	112	$2e-005$
90	60	245	$5e-005$
120	50	490	$1e-004$
150	45	1120	$2e-004$

$$\begin{aligned} \int_0^H \rho v_{z2}(y) x_2 \mathrm{d}y &= \int_0^H \rho v_{z1}(y) x_1 \mathrm{d}y, \\ \int_0^H \rho v_{z4}(y) x_4 \mathrm{d}y &= \int_0^H \rho v_{z3}(y) x_3 \mathrm{d}y. \end{aligned} \tag{10}$$

Therefore,

$$\frac{v_{z2}(y)}{v_{z1}(y)} = \frac{x_1}{x_2}, \tag{11}$$

$$\frac{v_{z3}(y)}{v_{z4}(y)} = \frac{x_4}{x_3}. \tag{12}$$

In order to make Equations (11) and (12) hold, $y \neq 0$. Equations (11) and (12) show that the velocity of the fluid in the z direction is inversely proportional to the width of the channel at the position of the convergent channel on the same side of the pin and the same height of the channel. Combing Equations (8) and (9), we can obtain

$$\begin{aligned} v_{z1}(y) &> v_{z2}(y), \\ v_{z3}(y) &> v_{z4}(y). \end{aligned} \tag{13}$$

Therefore, at the same screw channel height y, the velocity gradient of the fluid on both sides of the pin along the z direction exists. This quantitatively proves the conclusion that the qualitative analysis in Section 2.4 has elongational deformation.

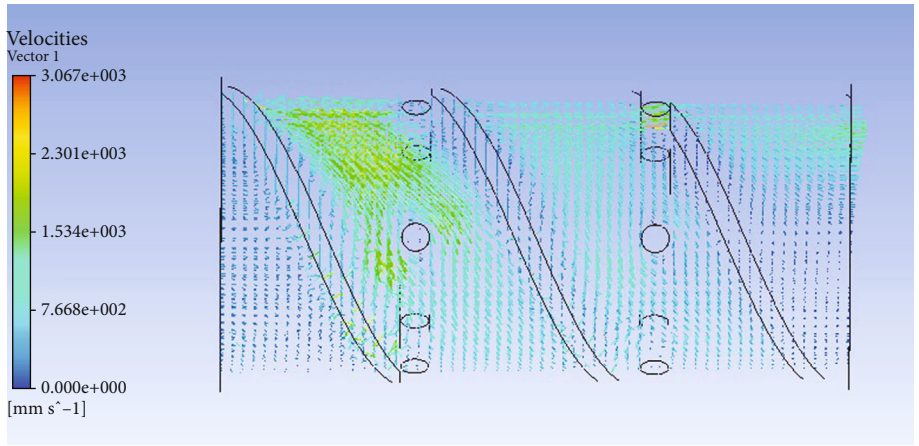

(a) Mixing section of the pin-barrel extruder

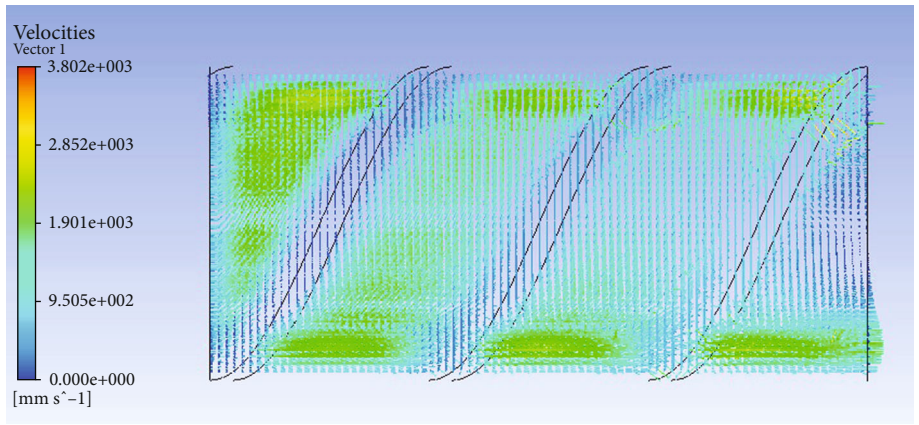

(b) Mixing section of the single screw extruder

Figure 6: Velocity vector nephogram of the mixing section (D = 150 *mm*).

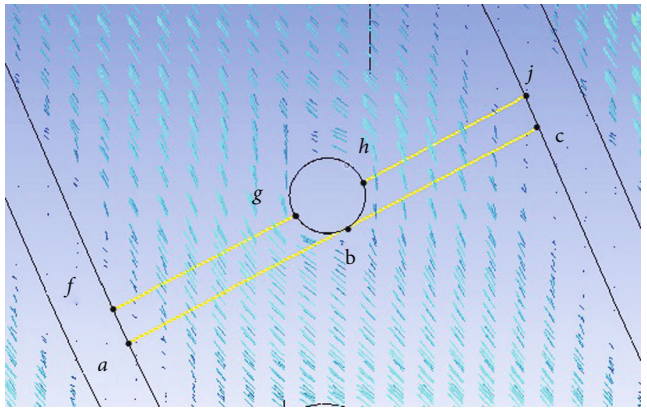

Figure 7: Flow field amplification near the pin.

2.6. Quantitative Calculation of Elongational Deformation. By multiplying the sides of Equation (11) and (12), respectively, and considering the inlet velocity in the critical state, $v_{z2}(y) = v_{z4}(y) = v_z(y)$, we can obtain

$$\frac{v_{z3}(y)}{v_{z1}(y)} = \frac{x_1 x_4}{x_2 x_3}. \tag{14}$$

As pins move in the region *pqsl*, $x_i (i = 1, 2, 3, 4)$ has been changing, resulting in $v_{z1}(y)$ and $v_{z3}(y)$ also changing. In order to obtain a simple analytical solution of elongational deformation, the relationship between the outlet velocity and the inlet velocity of the convergent channel on both sides of the pin must be known. Therefore, it is assumed that when the pin moves to a certain position in the analysis area, $v_{z1}(y) = v_{z3}(y)$, then $x_1 x_4 = x_2 x_3$, so

$$\frac{x_1}{x_2} = \frac{x_3}{x_4}. \tag{15}$$

When the center of the pin moves to the width of the normal screw channel of $W/2$, $x_1 = x_3$ and $x_2 = x_4$. Equation (15) holds, $v_{z1}(y) = v_{z3}(y)$, indicating that there is indeed such a point in the analysis area *pqsl* that satisfies the above hypothesis (as shown in position "2" in Figure 4).

From Equation (15),

$$\frac{x_1}{x_2} = \frac{x_3}{x_4} = \frac{x_1 + x_3}{x_2 + x_4} = \frac{W - d}{W}. \tag{16}$$

Combining Equations (11) and (12) and considering $v_{z1}(y) = v_{z3}(y)$, the relationship between the outlet velocity and inlet velocity at position "2" satisfying Equation (15)

can be obtained:

$$v_{z1}(y) = v_{z3}(y) = \frac{v_{z2}(y)W}{W-d} = \frac{v_{z4}(y)W}{W-d}. \quad (17)$$

Since $v_{z2}(y) = v_{z4}(y) = v_z(y)$ at the inlet of convergent channel on both sides of pin, so

$$v_{z1}(y) = v_{z3}(y) = \frac{W}{W-d} v_z(y). \quad (18)$$

It can be seen from Figure 4 that in the analysis region *pqsl*, the elongational deformation generated by the movement of the pin from position "1" to position "2" and from position "2" to position "3" is symmetrically equal to that at position "2." Therefore, in order to simplify the calculation, the elongational deformation of the fluid induced by the pin at the position "2" of Equation (15) can be used as the average value of the elongational deformation induced by the pin at any position in the screw channel during the rotation of the screw for a round. Therefore, according to the definition of elongational strain,

$$\dot{\varepsilon} = \frac{dv}{dz} \approx \frac{\Delta v}{d/2}. \quad (19)$$

From Equation (18),

$$\Delta v = v_{z1}(y) - v_z(y) = v_{z3}(y) - v_z(y) = \frac{d}{W-d} \cdot v_z(y). \quad (20)$$

Therefore,

$$\dot{\varepsilon} = \frac{2}{W-d} \cdot v_z(y). \quad (21)$$

Equation (21) shows that the elongational strain rate (s^{-1}) of the fluid on both sides of the pin will change due to the different height of the screw channel. And because

$$\dot{\varepsilon} = \frac{\mathrm{d}\varepsilon}{\mathrm{d}t} = \frac{\Delta\varepsilon}{\Delta t}, \quad (22)$$

combining Equation (21), the average elongational deformation $\Delta\varepsilon$ in one side (left or right side) of the pin at any pin position is

$$\Delta\varepsilon = \dot{\varepsilon} \cdot \Delta t = \frac{2}{W-d} \cdot v_z(y) \cdot \Delta t, \quad (23)$$

where

$$v_z(y) = \frac{v_b \cos\theta}{H} \cdot y = \frac{\pi DN \cos\theta}{H} \cdot y. \quad (24)$$

When the screw speed is N (rpm), the time of screw rotation 1r is $1/N$ (min). In the process of screw rotation 1r, the path length of a single pin is πD. For a single pin, the path of elongational deformation is $d/2$, and the time is $\Delta t(\mathrm{min})$, so

$$\frac{d/2}{\pi D} = \frac{\Delta t}{1/N}, \quad (25)$$

$$\Delta t = \frac{d}{2\pi DN}. \quad (26)$$

By substituting Equations (24) and (26) into Equation (23), it is found that the elongational deformation of fluid on one side of a single pin at the height of the screw channel y is

$$\Delta\varepsilon = \frac{d\cos\theta}{H(W-d)} \cdot y. \quad (27)$$

Therefore, the elongational deformation of the fluid on both sides of a single pin at the height of the screw channel y is

$$2\Delta\varepsilon = \frac{2d\cos\theta}{H(W-d)} \cdot y. \quad (28)$$

When $y = H/2$,

$$2\Delta\varepsilon_{H/2} = \frac{d\cos\theta}{W-d}. \quad (29)$$

By integrating Equation (28), $y \in (0, H)$, the total elongational deformation of fluid on both sides of a single pin in the whole screw channel depth is obtained as follows:

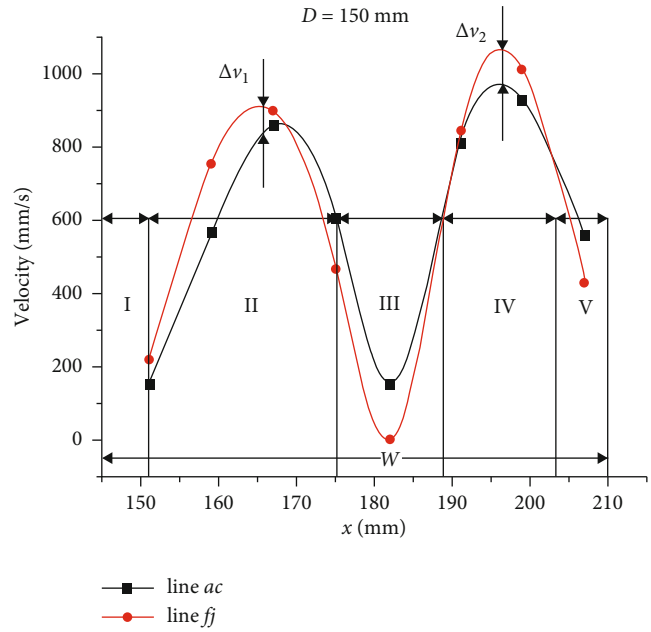

FIGURE 8: Velocity distribution of fluid layer at the position $y = H/2$ near the pin. (I: Region near the flight pushing side. II: Region of the left pin. III: Pin and region around the pin. IV: Region of the right pin. V: Region near the flight dragging side.)

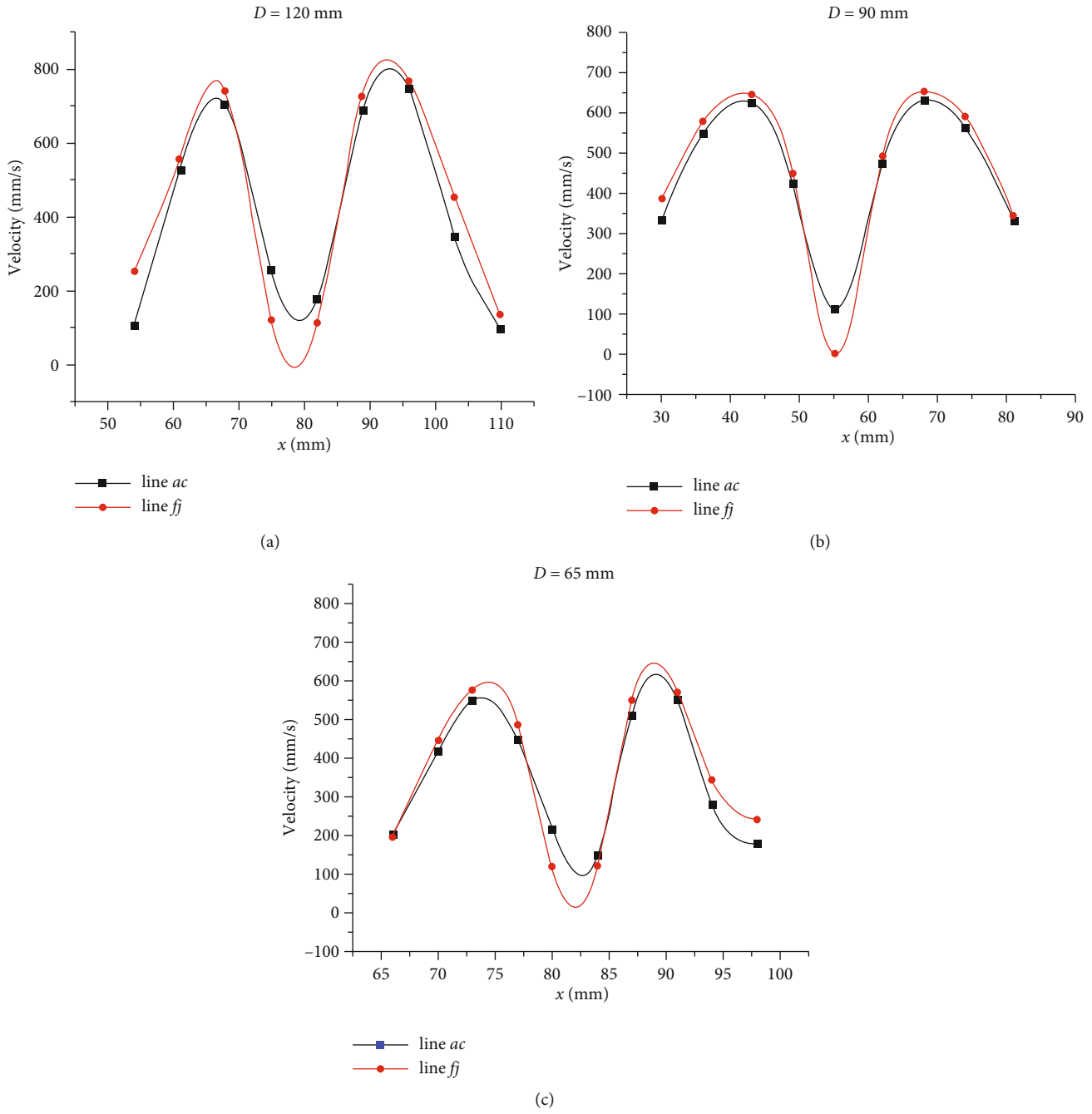

FIGURE 9: Velocity distribution of fluid layer of other screw specifications.

$$\varepsilon_{\frac{d}{2}} = \frac{dH\cos\theta}{W-d}. \tag{30}$$

It should be noted that in the screw flight slot section outside the analysis area $pqsl$ (z_s section in Figure 4), when the pin passes, elongational deformation occurs on the left (or right), both sides or right (or left) of the pin in the z direction. Since z_s is small, the elongational deformation in section z_s is still approximately calculated according to the above method.

When the screw rotates 1r, the number of elongational deformations produced by a single pin at $d/2$ distance is 2 $\pi D/d$. The total elongational deformation produced by a single pin is

$$\varepsilon_{\pi D} = \varepsilon_{d/2} \times \frac{2\pi D}{d} = \frac{2\pi HD\cos\theta}{W-d}. \tag{31}$$

Set the extruder has a total of m rows and each row has n pins. When the screw rotates 1r, the elongational deformation induced by all pins is

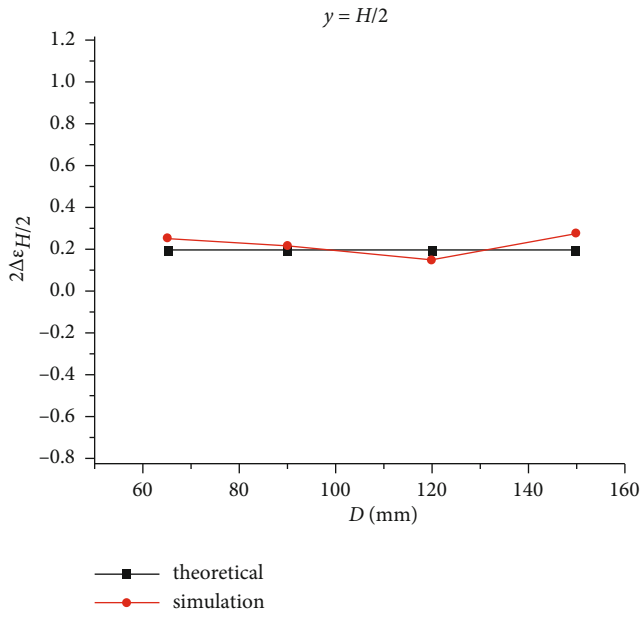

Figure 10: Elongational deformation of fluid on both sides of pin at $y = H/2$.

$$\varepsilon_{\Sigma,\pi D} = \frac{2mn\pi HD\cos\theta}{W-d}. \tag{32}$$

When the screw rotation numbers in unit time (s) is $N/60$, the elongational deformation of all pins in unit time (s) is

$$\varepsilon_{\Sigma} = \frac{mn\pi HDN\cos\theta}{30(W-d)}. \tag{33}$$

Equation (33) shows that the elongational deformation of all pins per unit time (s) depends on the screw diameter, helical angle, screw channel depth, normal screw channel width, pin diameter, pin number, and screw rotation speed.

According to the general design experience, the screw of the same specification has the following typical approximate relationship:

$$e \approx 0.07D,\ H \approx 0.2D,\ d \approx 0.1D,$$
$$W \approx \frac{\pi D\sin\theta}{i} - e. \tag{34}$$

In the above equation, i is the number of screw heads, and generally in pin barrel section, $i = 2$.

Substituting the above relation into Equation (31), we can get

$$\varepsilon_{\pi D} = \frac{\pi D\cos\theta}{1.25\pi\sin\theta - 0.425}. \tag{35}$$

Substituting Equation (34) into Equation (33), we also get

$$\varepsilon_{\Sigma} = \frac{mn\pi DN\cos\theta}{75\pi\sin\theta - 25.5}. \tag{36}$$

Equation (36) shows that for the pin-barrel cold-feed extruder with a given specification, D and θ are known quantities, and the main factors affecting the elongational deformation of pins per unit time are the screw rotation speed and the number of pins.

3. Simulation

The three-dimensional model of the mixing section of pin barrels was established [20, 25, 26], which is shown in Figure 5. The finite element simulation of the three-dimensional model was carried out by Polyflow, and the velocity vector nephogram in the simulation results was numerically analyzed. The parameter settings (according to the general screw design standard, the helical angle θ is set at 24° to allow for the fluctuation of pressure transfer and to achieve the desired pumping capacity) of the mixing sections are shown in Table 1.

In order to simplify the calculation, the following assumptions were made in the simulation: (i) The rubber compound is full of screw channels and incompressible. (ii) The influence of gravity and inertia force is ignored because of the large rubber melt viscosity. (iii) There is no wall slip. (iv) The rubber compound is laminar flow. (v) There is isothermal flow [14–18].

The Bird-Carreau equation was used for the constitutive model to describe the rheological characteristics of rubber compound:

$$\eta(\dot{\gamma}) = \eta_{\infty} + (\eta_0 - \eta_{\infty})\left[1 + (\lambda\dot{\gamma})^2\right]^{(n-1)/2}, \tag{37}$$

where η_{∞} is the infinite shear viscosity (Pa·s), η_0 is the zero shear viscosity (Pa·s), λ is the relaxation time (s), $\dot{\gamma}$ is the shear rate, and n is the non-Newtonian index.

The physical parameters of the rubber compound are as follows:

Table 2 shows the data satisfying Equation (37), where the standard errors of zero shear viscosity and relaxation time are minimized [19]. According to the general design standard of the screw, the screw diameter of each specification has different rotational speed ranges. In order to improve the authenticity and practicability of simulation results, the boundary conditions and rotational speed (Table 3) are selected as follows: (i) combined with the extrusion output of extruder and the typical ratio-gravity of rubber compound (1.25), the volume flow rate at the flow field inlet of the screw channel can be calculated (Table 3). (ii) Select free flow at the outlet of the flow field of the screw channel. (iii) The wall condition is set as no wall slip. (iv) Screw is the moving part.

Under the above conditions, CFD-POST was used to generate the velocity vector nephogram. For the convenience of observation, taking the screw of D = 150 *mm* as an example [21], the image is generated as shown in Figure 6.

4. Result Analysis

In the direction of the drag flow, by comparing the velocity vector of the fluid in the screw channel, it can be observed that the color of the fluid velocity vector changes obviously near the pin of the pin barrel extruder (Figure 6(a)); in the

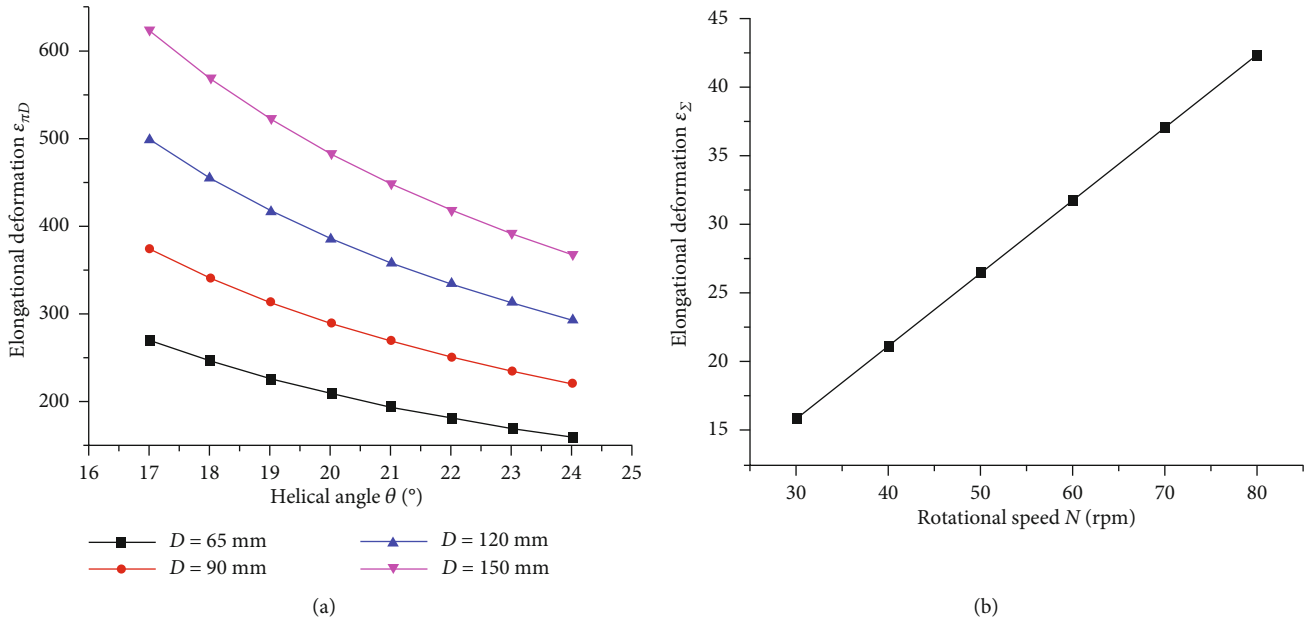

Figure 11: Numerical simulation of key factors affecting elongational deformation.

single screw extruder, the velocity vector of the fluid almost keeps the same color (Figure 6(b)). The velocity vector nephogram generated by simulation shows that in the pin-barrel extruder, the existence of pins indeed makes the fluid generate velocity gradient and elongational deformation in the direction of drag flow.

In order to clearly observe the fluid motion near the pin, the flow field near the pin in Figure 6 was enlarged. As shown in Figure 7, combined with the theoretical analysis in Section 2, the pin was selected as far as possible to move to the position that satisfies Equation (15). Then the fluid layers at the inlet and outlet when the screw channel depth $y = H/2$ are taken to calculate the velocity $v_z(H/2)$ of the rubber compound on this fluid layer, as shown in Figure 8.

The fluid layer velocity of other specifications of the screw is shown in Figure 9.

According to Figures 8 and 9, the velocities of the region I, III, and V were ignored. The maximum velocity difference Δv_1 and Δv_2 of the fluid on both sides of the pin are taken, and then, the average velocity difference $\overline{\Delta v} = (\Delta v_1 + \Delta v_2)/2$ was calculated. Using Equations (19) and (22), the elongational deformation simulation values of the fluid on both sides of the pin were obtained when $y = H/2$. The theoretical values were calculated according to Equation (29), as shown in Figure 10.

By observing Figure 10, it can be clearly seen that the simulated value and the theoretical value are approximately consistent, indicating that the theoretical analysis in Section 2 is approximately correct and can be used for practical calculation. In order to investigate the key factors affecting the elongational deformation, condition (a) was substituted into Equation (35), and condition (b) was substituted into Equation (36) for numerical simulation. The effects of screw diameter D, helical angle θ, and rotational speed N on the elongational deformation were analyzed, and the results are shown in Figure 11.

(a) Screw diameter: $D \in (60\text{ mm}, 150\text{ mm})$

(i) Helical angle: $\theta \in (17^\circ, 24^\circ)$

(b) Number of pins: $m = 2$, $n = 6$.

(i) Screw diameter: $D = 65$ mm

(ii) Helical angle: $\theta = 24^\circ$

(iii) Rotational speed: $N \in (30\text{ rpm}, 80\text{ rpm})$

It can be seen from Figure 11(a) that when the screw diameter is constant, the elongational deformation will gradually decrease with the increase of the helical angle. When the helical angle is constant, the elongational deformation increases with the increase of screw diameter. It also can be seen from Figure 11(b) that when the screw specification is given, the elongational deformation induced by pins in unit time will increase linearly with the increase of the screw rotational speed.

5. Conclusion

Through simple flow field and geometric simplification, the mathematical model was established to prove and quantitatively calculate the elongational deformation induced by pins. The mathematical model in the theoretical analysis was verified

by simulating the flow field in the mixing section, and it was found that the simulated value of elongational deformation was approximately consistent with the theoretical value. According to the mathematical model and simulation results of elongational deformation, the following conclusions can be drawn that the elongational deformation will gradually increase with the increase of screw diameter. For the screw of the same specification, the increasing helical angle will reduce the elongational deformation, and the increasing rotational speed will linearly increase the elongational deformation in unit time.

Although the model is used for the rough estimation of elongational deformation, it reflects the key factors affecting the elongational deformation induced by pins. We can also approximately estimate the mixing performance of an extruder according to the calculated elongational deformation value, so as to make a more convenient and intuitive comparison. This theory can be used to establish the complete mixing theory model of pin-barrel cold-feed extruder.

Nomenclature

v_b: Moving speed of the barrel
D: Screw diameter
N: Screw rotational speed
v_x: Cross-channel velocity
v_z: Down-channel velocity
τ: Stress tensor
η: Newton viscosity
E: Strain rate tensor
∇: Differential operator
v: Velocity vector
ρ: Density
P: Pressure
g: Gravity acceleration
H: Screw channel depth
θ: Helical angle
d: Pin diameter
W: Normal screw channel width
e: Normal screw flight width
z_s: Screw flight slot length
$\dot{\varepsilon}$: Elongational strain
$\Delta\varepsilon$: Elongational deformation
i: Screw heads
η_∞: Infinite shear viscosity
η_0: Zero shear viscosity
λ: Relaxation time
$\dot{\gamma}$: Shear rate
n: Non-Newtonian index.

Data Availability

The data used to support the findings of this study are included within the article.

Conflicts of Interest

The authors declare that they have no conflicts of interest.

Acknowledgments

This study was supported by the Science and Technology Innovation Project of Shandong Province of China (Grant No. 2020CXGC010312). Furthermore, the authors would like to thank the Associate Professor Liu Yanchang and Dr. Pan for their discussions and guidance throughout this work.

References

[1] W. G. Yao, K. Takahashi, K. Koyama, and G. C. Dai, "Design of a new type of pin mixing section for a screw extruder based on analysis of flow and distributive mixing performance," *Chemical Engineering Science*, vol. 52, no. 1, pp. 13–21, 1997.

[2] S.-P. Rwei, "Distributive mixing in a single-screw extruder—-evaluation in the flow direction," *Polymer Engineering & Science*, vol. 41, no. 10, pp. 1665–1673, 2001.

[3] C. Rauwendaal, "Mixing in single-screw extruders," *Mixing (Second Edition)*, pp. 853–945, 2009.

[4] W. D. Mohr, R. L. Saxton, and C. H. Jepson, "Theory of mixing in the single-screw extruder," *Industrial and Engineering Chemistry*, vol. 49, no. 11, pp. 1857–1862, 1957.

[5] J. Wang, "Influence of helical grooved structure on mixing process in a single screw extruder," *Key Engineering Materials*, vol. 561, no. 561-561, pp. 212–217, 2013.

[6] Y. Yabushita, R. Brzoskowski, J. L. White, and N. Najakima, "Flow of rubber compound in a pin barrel screw extruder," *International Polymer Processing*, vol. 4, no. 4, pp. 219–224, 1989.

[7] K.-C. Shin and J. L. White, "Basic studies of extrusion of rubber compounds in a pin barrel extruder," *Rubber Chemistry and Technology*, vol. 66, no. 1, pp. 121–138, 1993.

[8] R. Brzoskowski, J. L. White, W. Szydlowski, N. Nakajima, and K. Min, "Modelling flow in pin-barrel screw extruders," *International Polymer Processing*, vol. 3, no. 3, pp. 134–140, 1988.

[9] V. Schöppner, M. Schadomsky, C. Hopmann, and F. Lemke, "Investigations of the mixing behaviour of pin-type rubber extruders," in *PROCEEDINGS OF PPS-31: The 31st International Conference of the Polymer Processing Society–Conference Papers*, p. 130003, Chengdu International Convention and Exhibition Center, 2016.

[10] L. Erwin, *Theory of mixing sections in single screw extruders*, vol. 18, no. 7, 1978John Wiley & Sons, Ltd, 1978.

[11] W. G. Yao, K. Takahashi, and Y. Abe, "Analytical study on flow and distributive mixing of a new type pin mixing section for screw extruder," *International Polymer Processing*, vol. 11, no. 3, pp. 222–227, 1996.

[12] N. Domingues, A. Gaspar-Cunha, and J. A. Covas, "Modelling of mixing in single screw extruders," *Materials Science Forum*, vol. 514-516, no. 514-516, pp. 1409–1413, 2006.

[13] Y. Wang and C. T. Cheng, "Non-Newtonian flow modeling in the mixing section of a single-screw extruder with flow analysis network method," *Polymer Engineering and Science*, vol. 36, no. 5, pp. 643–650, 1996.

[14] K. C. Shin and J. L. White, "Simulation of non-Newtonian flow of rubber compounds in a pin barrel screw extruder," *Rubber Chemistry and Technology*, vol. 70, no. 2, pp. 264–270, 1997.

[15] T. Kumazawa, R. Brzoskowski, and J. L. White, "Simulation of non-isothermal flow in a pin barrel cold feed extruder,"

Kautschuk Gummi Kunststoffe, vol. 43, no. 8, pp. 688–691, 1990.

[16] A. Ahmadian, Y. Tamsilian, and R. Ahmad, "Viscoelastic and generalized Newtonian fluid flows simulation in single screw extruder using computational flow dynamics," *EPF*, 2011.

[17] W. Jian and G. Di, "Numerical simulation study on effect of barrel structures on performance of single screw extruder," *Plastics Science and Technology*, vol. 40, no. 10, pp. 74–78, 2012.

[18] G. Bhme and J. Broszeit, "Numerical flow simulation for Bingham plastics in a single-screw extruder," *Theoretical and Computational Fluid Dynamics*, vol. 9, no. 1, pp. 65–74, 1997.

[19] J. Chen, P. Dai, H. Yao, and T. Chan, "Numerical analysis of mixing performance of mixing section in pin-barrel single-screw extruder," *Journal of Polymer Engineering*, vol. 31, no. 1, 2011.

[20] B. Chao and J. Bo, "Study of residence time distribution in a reciprocating single-screw pin- barrel extruder," *Journal of Materials Processing Technology*, vol. 209, no. 8, pp. 4147–4153, 2009.

[21] X. Wei, L. Hong, D. Wang, C. Guo, and J. Wu, *Numerical simulation of flow fields in pin barrel extruder*, China Synthetic Rubber Industry, 2006.

[22] M. A. Huneault, M. F. Champagne, and A. Luciani, "Polymer blend mixing and dispersion in the kneading section of a twin-screw extruder," *Polymer Engineering & Science*, vol. 36, no. 12, pp. 1694–1706, 1996.

[23] J. M. Buick and J. A. Cosgrove, "Numerical simulation of the flow field in the mixing section of a screw extruder by the lattice Boltzmann model," *Chemical Engineering Science*, vol. 61, no. 10, pp. 3323–3326, 2006.

[24] H. Horiguchi, K. Takahashi, and T. Yokota, "Numerical simulation of the flow field in the mixing section of a screw extruder by the lattice gas automata method," *Journal of Chemical Engineering of Japan*, vol. 36, no. 1, pp. 110–113, 2003.

[25] S. K. Singh and K. Muthukumarappan, "Rheological characterization and CFD simulation of soy white flakes based dough in a single screw extruder," *Journal of Food Process Engineering*, vol. 40, no. 2, 2017.

[26] Union E, *CFD Simulation of Rotational Barrel Segment Mixing Performance in Single Screw Extruder*, 2019.